Molecular Crystals and Liquid Crystals

Publication details, including instructions for authors and subscription information:
http://www.tandfonline.com/loi/gmcl20

Theory, Measurement, and Origin of Optical Activity in Benzil Crystal

Jan Říha [a], Ivo Vyšín [a] & Hana Lapšanská [a]

[a] Department of Theoretical Physics, Palacký University, Olomouc, Czech Republic

Version of record first published: 31 Aug 2006

To cite this article: Jan Říha, Ivo Vyšín & Hana Lapšanská (2005): Theory, Measurement, and Origin of Optical Activity in Benzil Crystal, Molecular Crystals and Liquid Crystals, 442:1, 181-201

To link to this article: http://dx.doi.org/10.1080/154214090964889

Mol. Cryst. Liq. Cryst., Vol. 442, pp. 181–201, 2005

ISSN: 1542-1406 print/1563-5287 online
DOI: 10.1080/154214090964889

Taylor & Francis
Taylor & Francis Group

Theory, Measurement, and Origin of Optical Activity in Benzil Crystal

Jan Říha
Ivo Vyšín
Hana Lapšanská
Department of Theoretical Physics, Palacký University,
Olomouc, Czech Republic

The three coupled oscillator model and its application to the explanation of optical-rotatory dispersion and circular dichroism of benzil crystal is discussed. The previously measured experimental data are approximated by the theoretical set of formulas provided by this model. The twelve-term formula, which was computed using our computer program, is derived from the interpretation of the optical-rotatory dispersion of benzil. Similarly, the circular-dichroism data are analyzed. Both the previously published experimental data and the latest measurements are used for this reason. The obtained results are compared and discussed with respect to the origin of the optical activity occurring in benzil crystal.

Keywords: benzil; circular dichroism; coupled oscillators; optical activity; optical-rotatory dispersion

INTRODUCTION

The optical activity of crystals has two aspects that arise from the interaction of the radiation with the matter—dispersive and absorptive. The first aspect is the optical-rotatory dispersion, which means the dependency of the rotation of the linear polarized wave per unit length on the frequency ω or on the wavelength λ. The second aspect is the circular dichroism, which is defined as the dependency of the ellipticity per unit length of the wave radiating from the crystal on ω or on λ.

These effects are based on the fact that the linearly polarized wave is split into two circularly polarized waves in the optically active

Address correspondence to Jan Říha, Department of Theoretical Physics, Palacký University, 17. Listopadu 50, 77200 Olomouc, Czech Republic. E-mail: riha@risc.upol.cz

medium—into the left and the right circularly polarized waves. These waves propagate through the optically active medium with different velocities, and they are also absorbed differently. It means that the optically active medium is characterized by different refractive indices for these waves. The complex rotatory power $\bar{\rho}$ is used as the characteristic of the medium and it is defined by the relation

$$\bar{\rho} = \rho + i\sigma = \frac{\omega}{2c}(\bar{n}_l - \bar{n}_r) = \frac{\omega}{2c}[(n_l - n_r) + i(\kappa_l - \kappa_r)], \tag{1}$$

where ρ is the optical rotatory dispersion and σ is the circular dichroism. The quantities n_l, n_r and κ_l, κ_r are the real and imaginary parts of the complex refractive indices $\bar{n}_l$ and $\bar{n}_r$ of the medium for the left and the right circularly polarized waves. It is known that the optical-rotatory dispersion and the circular dichroism as the dispersive and the absorptive aspects are connected by the Kramers–Kronig transforms:

$$\rho(\lambda) = \frac{2}{\pi}\int_0^\infty \frac{\Lambda\sigma(\Lambda)}{\lambda^2 - \Lambda^2}d\Lambda, \tag{2}$$

$$\sigma(\lambda) = -\frac{2}{\pi\lambda}\int_0^\infty \frac{\Lambda^2\rho(\Lambda)}{\lambda^2 - \Lambda^2}d\Lambda. \tag{3}$$

Benzil belongs to the small class of molecules that are not optically active in solution but that gain their optical activity in only the crystalline state. The molecules are arranged in a helical form and they can be translated from one to the other by a trigonal screw axis. The position of molecules can be given by both the left-hand screw and the right-hand screw. The optical activity of benzil is due to the additional asymmetry obtained in the helical structure.

The crystal structure of benzil ($C_6H_5 \cdot CO \cdot CO \cdot C_6H_5$) was determined by Allen [1], Banerjee and Sinha [2], and also Brown and Sadanga [3]. Later, a complete determination of the structure was made. Benzil crystallizes in the trigonal trapezohedral class with the space group of symmetry D_3^4 or D_3^6. The other typical representatives of this space group are α-quartz, cinnabar, tellurium, selenium, and camphor. The optical activity of these crystals has the crystalline origin; the only exception is camphor, which is optically active also in solution.

The crystal of benzil is built upon a hexagonal lattice and the unit cell accommodates three molecules disposed spirally around the trigonal axis. Although benzil exhibits no optical activity in solution, the molecules may be expected to be optically active because they have

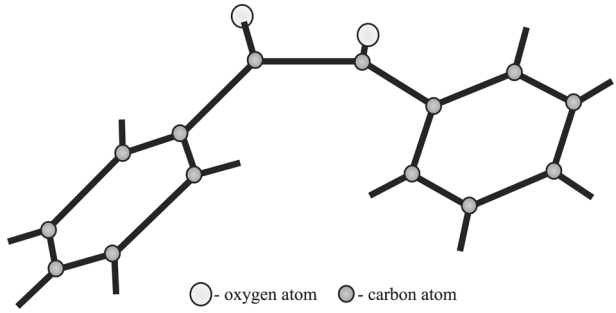

FIGURE 1 Configuration of benzil molecule.

a skew configuration. The α-diketone moiety of the benzil molecule is twisted (O=C−C=O torsion angle is 108.8°), whereas the benzoyl groups are nearly planar (O=C−C=C torsion angles are −4.0° in both cases) [4]; see Figure 1.

The optical-rotatory dispersion of benzil was measured by Chandrasekhar [5] for the first time for wavelengths ranging from 0.360 μm to 0.900 μm at the temperature of 300 K. The detailed experimental data in the wavelength region from 0.400 μm to 0.630 μm were obtained by Kizel, Krasilov, and Shamraev [6] at the same temperature. The optical-rotatory dispersion curve was approximated by the sum of terms provided by [7]:

$$\rho(\lambda) = \sum_i \frac{K_i^{(\lambda)}(\lambda^2 - \lambda_i^2)}{(\lambda^2 - \lambda_i^2)^2 + \Gamma_i^2 \lambda^2}, \tag{4}$$

where λ_i are the central dichroic wavelengths, Γ_i the damping constants, and $K_i^{(\lambda)}$ the constants proportional to the rotational strengths of the corresponding wavelength bands. Their result is noted in Table 1. However, a comparison of this result with the experimental data shows a considerable inaccuracy in the 0.340 μm–0.420 μm region. This fact is well manifested by Figure 2, where the experimental data and the theoretical curve from Table 1 are graphed.

The experimental data of circular dichroism of benzil crystal were provided by Chaudhury and El-Sayed [8] at 77 K in the direction of the optical axis. They found two strong bands with the maxima at 0.3325 μm and 0.385 μm and an extremely weak band with an unresolved maximum at 0.425 μm. The more accurate measurement of Perekalina et al. [9] in the 0.340 μm–0.500 μm region showed the possibility of the band with the maximum in the close vicinity of 0.3325 μm. However, the maximum of the second strong band lies at

TABLE 1 Approximation of Experimental Data by Eq. (4) [9], $G = \sqrt{S/N} = 39.0\,\text{deg} \cdot \text{mm}^{-1}$

i	λ_i (μm)	K_i	Γ_i (μm)
1	0.309	8.03	0.012
2	0.331	0.60	0.016
3	0.336	−2.07	0.021
4	0.346	0.81	0.016
5	0.380	−0.33	0.021
6	0.398	−1.11	0.016

0.398 μm. The existence of the third weak peak was not confirmed. Recently Moxon, Renshaw, and Tebbutt [11] addressed the problem of measurement of the circular dichroism of benzil. This measurement is consistent with those of Perekalina et al. [9] with the advantage that Moxon, Renshaw, and Tebbutt's results were obtained simultaneously for the circular dichroism and optical-rotatory dispersion in one experiment. The last experimental study of the benzil-crystal optical activity was made by Polonski et al. [12]. They compared the circular dichroism spectra of the benzil crystalline inclusion complexes with cholic and deoxycholic acids.

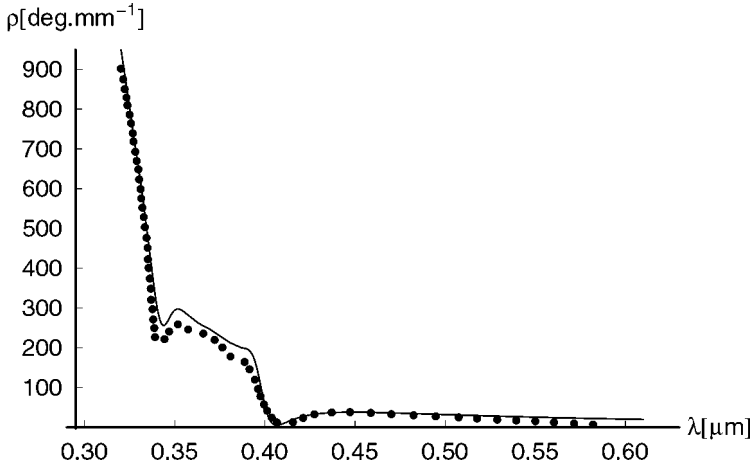

FIGURE 2 Optical-rotatory dispersion curve given by Table 1 in comparison with Kizel et al.'s [10] optical-rotatory dispersion experimental data of benzil crystal (points).

It is shown that the complete set of formulas for the optical-rotatory dispersion given by our theoretical computations for the crystals belonging to the space groups D_3^4 or D_3^6 can satisfactorily fit experimental data not only in the immediate vicinity of the absorption band but also in the wavelength region, where the Cotton effect occurs. The obtained optical-rotatory dispersion formula is used to create the circular-dichroism formula based on the connection of the optical-rotatory dispersion and circular dichroism by the Kramers–Kronig transforms (2), (3). This theoretical circular-dichroism curve is compared with the available experimental data [9,12].

THEORY

We intend to use the theory of the optical activity based on the model of coupled oscillators, where molecules or atoms in the crystal structure are represented by linear harmonic oscillators. The primary Chandrasekhar model of two coupled oscillators [13] has been generalized, as it seems to contain two problems that should be solved in the optical activity of crystals with space groups of symmetry D_3^4 and D_3^6.

The Chandrasekhar model includes only the couplings between the adjacent oscillators on the helix. However, in the practical cases, where the diameter of the helix is comparable with the height of the elementary cell, the distances between even or odd oscillators are comparable with the distances between adjacent oscillators, and therefore the couplings between the even or odd oscillators on the helix can result in the substantial influence on the optical activity. Furthermore, the groups of coupled oscillators are not independent as in the Chandrasekhar model. In the model of two coupled oscillators, the second oscillator of any couple of coupled oscillators is at the same time the first oscillator of the next couple and the same conclusion holds for the couplings between even or odd oscillators.

The description of the crystalline optical activity based on the model of coupled oscillators can use the Drude–Sellmaier dispersion theory of the refractive indices of the medium (represented by the coupled oscillators) for the left and the right circularly polarized waves. The resulting expressions of these refractive indices can be substituted in the relation (1) for the complex rotatory power followed by a derivation of the optical-rotatory dispersion and circular dichroism. The problem can be solved, as in the Chandrasekhar model, using the normal coordinates. The characteristic frequencies of single oscillators are split into n frequencies of the normal modes of vibrations, where n is the number of coupled oscillators forming one compound oscillator in the model. The oscillator strengths of the normal modes are used as

the characteristics of the normal modes. Differences between the frequencies of normal modes and the corresponding characteristic frequency depend on the coupling constants of the couplings between oscillators. These coupling constants are presumed to be small. Therefore, the final results can be expressed (in any proper approximation of the oscillator strengths of the normal modes) in the dependency on the characteristic frequency of the single oscillator. Using this procedure, the results of the models of a different number of coupled oscillators can be compared. The basic approximation of the oscillator strengths of normal modes (it is shown that this approximation is valid for tellurium) is the strict approximation of the linear harmonic oscillator in which the oscillator strengths of the normal modes are equal.

Using this general procedure, the optical activity based on the models of three, four, five, and so on coupled oscillators was solved [14]. It was proven that the effects of the couplings between adjacent oscillators can be held as additive when the terms containing higher powers of the small coupling constant Q are not taken into account. For example, one compound oscillator consisting of three coupled oscillators on the helix (but including the couplings only between adjacent oscillators) leads to a two-fold optical activity in comparison with two coupled oscillators if the terms of the order Q^2 are neglected. The models of three, four, five, and so on. coupled oscillators, when the couplings among adjacent, even, and odd oscillators are considered, were solved, and also the additivity of the coupling effects between even or odd oscillators was proven. The model of three coupled oscillators is the lowest model, which can include couplings between even or odd oscillators, except the couplings between adjacent oscillators. Taking $N/2$ as the number of such compound oscillators in the volume unit ($N$is the number of single oscillators), all couplings between adjacent oscillators and half of the couplings between even and odd oscillators are considered. However, the couplings' effects are additive, and the couplings between all even and all odd oscillators on one helix can be included very simply—by doubling the constant of the coupling between even or odd oscillators in the final relations for the optical-rotatory dispersion and circular dichroism. The accuracy of this model (up to and including the terms containing the square of the coupling constants) seems to be satisfactory for the real optically active crystals.

It should be noted that the influence on the optical activity of other possible couplings between the oscillators lying on one helix can be neglected for the crystals with the space groups of symmetry D_3^4 and D_3^6. The direction of vibrations of any oscillator on the helix (oscillator number one) and the oscillator number four with respect to number

one is accidentally oriented, and therefore the coupling between them does not lead to the optical activity. The oscillators number one and number five are too distant, and consequently the coupling between them is negligible in comparison with the coupling between the adjacent oscillators, which gives the optical activity of the same type. Also, the couplings between the oscillators lying on the different helices are usually neglected in the models of coupled oscillators. These oscillators are somewhat more distant than the adjacent oscillators on one helix and above all, the type of the couplings between the oscillators on one helix is different from the type of the couplings between the oscillators on different helices in many cases.

The following model of three coupled oscillators is used. For the description of the optical activity let us consider three oscillators, each of which has the mass m and the charge e, that lie on the helix, the axis of which (the crystal axis c) is parallel with the z coordinate axis. The second oscillator lies in the plane $z = 0$, its coordinates are $x, y, 0$, and its direction of vibrations is described by the direction cosines α, β, γ. The first oscillator lies on the helix in the plane $z = -d$ and its direction of vibrations is rotated by the angle $-\theta$ around the z axis with respect to the second one. Similarly, the third oscillator lies on the helix in the plane $z = d$ and its direction of vibrations is turned by the angle $+\theta$ around the z axis with respect to the second one. The angle θ is of course 120° for the crystals belonging to the space groups of symmetry D_3^4 and D_3^6. All oscillators are assumed to be identical. In addition, the optical activity only in the direction of the crystal axis where the optical activity is not screened by the birefringence is studied. The positions of oscillators are illustrated in Figure 3.

The preceding plane electromagnetic wave of the wave vector $\vec{k}$, parallel to the z axis, and the angular frequency $\omega = ck$ interacts with a quantum mechanical system. The Hamiltonian of this system can be written

$$\hat{H} = \frac{1}{2m}\left[\hat{\vec{p}} - q\hat{\vec{A}}(\vec{r}, t)\right]^2 + \hat{V}(\vec{r}), \tag{5}$$

where $\hat{\vec{p}}$ is the total momentum operator of all electrons in the system, $\hat{\vec{A}}$ is the operator of vector potential, q is the electric charge of the system, $\hat{V}(\vec{r})$ is the potential operator, and the vector $\vec{r}$ includes all coordinates describing the system.

The Hamiltonian equation (5) can be split into two parts:

$$\hat{H} = \hat{H}_0 + \hat{H}_{\text{int}}(t), \tag{6}$$

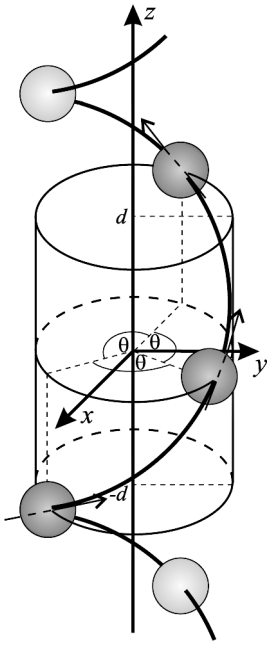

FIGURE 3 Scheme of the three-coupled oscillator model. The vibration directions of oscillators are described by arrows.

where $\widehat{H}_0$ is the Hamiltonian of the quantum mechanical system without incidence of the electromagnetic wave and $\widehat{H}_{\mathrm{int}}(t)$ is the interaction Hamiltonian with the incident wave.

The first part $\widehat{H}_0$ satisfies the relation

$$\widehat{H} = \frac{\hat{\vec{p}}^2}{2m} + \widehat{V}(\vec{r}). \tag{7}$$

The interaction Hamiltonian can be reduced at the low-intensity limit to the form [15]

$$\widehat{H}_{\mathrm{int}}(t) = -\frac{q}{m}\hat{\vec{p}} \cdot \hat{\vec{A}}. \tag{8}$$

The operator $\hat{\vec{A}}$ can be replaced by the classical expression

$$\vec{A} = \vec{A}_0 \mathrm{e}^{\mathrm{i}(kz-\omega t)} + \vec{A}_0^* \mathrm{e}^{-\mathrm{i}(kz-\omega t)} = \vec{A} = \vec{A}_0 \mathrm{e}^{\mathrm{i}(kz-\omega t)} + \mathrm{h.c.}, \tag{9}$$

where $\vec{A}_0$ is a complex vector constant, the symbol * denotes the complex conjugate quantity, and the abbreviation "h.c." means a

hermitian conjugate part. Then, the electric field vector is

$$\vec{E} = -\frac{\partial \vec{A}}{\partial t} = \vec{E}_0 e^{i(kz-\omega t)} + \text{h.c.}; \tag{10}$$

hence,

$$\vec{A} = -\frac{i}{\omega}\vec{E}_0 e^{i(kz-\omega t)} + \text{h.c.} = -\frac{i}{\omega}\vec{E}. \tag{11}$$

Therefore, the Hamiltonian for one compound oscillator, which contains three coupled oscillators, in the field of the left and the right circularly polarized waves has the form

$$\begin{aligned}\widehat{H}^{l,r} = &-\frac{\hbar^2}{2m}\sum_{\xi=1}^{3}\frac{\partial^2}{\partial r_\xi^2} + \frac{m\omega_0^2}{2}\sum_{\xi=1}^{3} r_\xi^2 + [\mu_1(r_1r_2 + r_2r_3) + \mu_2 r_1 r_3] \\ &+ \left(\frac{ie}{m\omega}\sum_{\xi=1}^{3} E_\xi^{l,r}\widehat{p}_\xi e^{\gamma_0 t} + \text{h.c.}\right),\end{aligned} \tag{12}$$

where r_1, r_2, r_3 are the displacements of the oscillators from their equilibria, $\mu_1(r_1r_2 + r_2r_3) + \mu_2 r_1 r_3$ is the potential energy of mutual interactions of the oscillators, the connection with the previously mentioned coupling constant Q is provided by the relation $\mu_1 = \frac{Q}{m}$, e is the charge of electron, and $E_\xi^{l,r}$ and $\xi = 1, 2, 3$ are the electric-field vectors of the left and the right circularly polarized waves. The upper indices l, r hold for the left and the right circularly polarized waves and $\widehat{p}_\xi$ are the momentum operators of all single oscillators. The small positive parameter γ_0 gives the possibility of adiabatic interaction at the time $t = -\infty$. This parameter γ_0 describes the damping following from the limited lifetime of oscillators in their excited states [16].

The problem is solved in normal coordinates q_1, q_2, q_3, which are connected with coordinates r_1, r_2, r_3 by the following transformation relations [17]

$$\begin{aligned} r_1 &= \frac{1}{\sqrt{2 + A_1^2}}\, q_1 + \frac{1}{\sqrt{2}} q_2 + \frac{1}{\sqrt{2 + A_3^2}}\, q_3, \\ r_2 &= \frac{A_1}{\sqrt{2 + A_1^2}}\, q_1 + \frac{A_3}{\sqrt{2 + A_3^2}}\, q_3, \\ r_3 &= \frac{1}{\sqrt{2 + A_1^2}}\, q_1 - \frac{1}{\sqrt{2}}\, q_2 + \frac{1}{\sqrt{2 + A_3^2}}\, q_3, \end{aligned} \tag{13}$$

where

$$A_1 = \frac{-\mu_2 + \sqrt{\mu_2 + 8\mu_1^2}}{2},\ A_2 = \frac{-\mu_2 - \sqrt{\mu_2 + 8\mu_1^2}}{2}. \tag{14}$$

The Drude–Sellmaier theory of the dispersion of refractive indices for the left and the right circularly polarized waves was used. The computation of the difference between complex refractive indices $\overline{n}_l - \overline{n}_r$ is possible, and with regard to Eq. (1), we obtain the optical rotatory dispersion

$$\rho(\omega) = A\omega^2 \sum_k \left\{ \frac{K_{k0}^{(1)}(\omega_{k0}^2 - \omega^2)}{(\omega_{k0}^2 - \omega^2)^2 + 4\gamma_0^2\omega^2} + \frac{K_{k0}^{(2)}[(\omega_{k0}^2 - \omega^2)^2 - 4\gamma_0^2\omega^2]}{[(\omega_{k0}^2 - \omega^2)^2 + 4\gamma_0^2\omega^2]^2} + \frac{K_{k0}^{(3)}(\omega_{k0}^2 - \omega^2)[(\omega_{k0}^2 - \omega^2)^2 - 12\gamma_0^2\omega^2]}{[(\omega_{k0}^2 - \omega^2)^2 + 4\gamma_0^2\omega^2]^3} \right\}, \tag{15}$$

and the circular dichroism

$$\sigma(\omega) = 2A\gamma_0\omega^3 \sum_k \left\{ \frac{K_{k0}^{(1)}}{(\omega_{k0}^2 - \omega^2)^2 + 4\gamma_0^2\omega^2} + \frac{2K_{k0}^{(2)}(\omega_{k0}^2 - \omega^2)}{[(\omega_{k0}^2 - \omega^2)^2 + 4\gamma_0^2\omega^2]^2} + \frac{K_{k0}^{(3)}[3(\omega_{k0}^2 - \omega^2)^2 - 4\gamma_0^2\omega^2]}{[(\omega_{k0}^2 - \omega^2)^2 + 4\gamma_0^2\omega^2]^3} \right\}, \tag{16}$$

where ω_{k0} is the frequency of the quantum transition from the ground state $|0\rangle$ to any excited state $|k\rangle$, $A = 4\pi N d e^2/mc^2(\alpha^2 + \beta^2)\sin\theta$ (N is the number of single oscillators in the volume unit), and the constants in the numerators are

$$\begin{aligned}
K_{k0}^{(1)} &= -\frac{2\cos\theta + A_1}{2 + A_1^2} f_{q_{1k0}} + f_{q_{2k0}}\cos\theta - \frac{2\cos\theta + A_3}{2 + A_3^2} f_{q_{3k0}}, \\
K_{k0}^{(2)} &= \frac{\mu_1}{m}\left[-\frac{2\cos\theta + A_1}{2 + A_1^2} A_3 f_{q_{1k0}} + \frac{\mu_2}{\mu_1} f_{q_{2k0}}\cos\theta - \frac{2\cos\theta + A_3}{2 + A_3^2} A_1 f_{q_{3k0}} \right], \\
K_{k0}^{(3)} &= \left(\frac{\mu_1}{m}\right)^2 \left[-\frac{\mu_2}{\mu_1}\frac{2\cos\theta + A_1}{2 + A_1^2} A_1 f_{q_{1k0}} \right. \\
&\quad \left. -2 f_{q_{2k0}}\cos\theta - \frac{\mu_2}{\mu_1}\frac{2\cos\theta + A_3}{2 + A_3^2} A_3 f_{q_{3k0}} \right].
\end{aligned} \tag{17}$$

The symbols $f_{q_{\eta k0}}$, $\eta = 1, 2, 3$, represent the oscillator strengths of normal modes of vibrations

$$f_{q_{\eta k0}} = \frac{2m\omega_{\eta k0}|\langle \eta_k | q_\eta | \eta_0 \rangle|^2}{\hbar}; \tag{18}$$

$\omega_{\eta k0}$ are the transition frequencies of normal modes of vibrations.

For the practical usage in the approximation of the optical-activity experimental data, the dependency on the wavelengths λ is usually used. Rewriting the optical-rotatory dispersion and circular dichroism equations (15) and (16) in this dependency, we obtain

$$\rho(\lambda) = \sum_k \left\{ \frac{K^\rho_{1k}(\lambda^2 - \lambda_k^2)}{(\lambda^2 - \lambda_k^2)^2 + \Gamma_k^2\lambda^2} + \frac{K^\rho_{2k}\lambda^2[(\lambda^2 - \lambda_k^2)^2 - \Gamma_k^2\lambda^2]}{[(\lambda^2 - \lambda_k^2)^2 + \Gamma_k^2\lambda^2]^2} + \frac{K^\rho_{3k}\lambda^4(\lambda^2 - \lambda_k^2)[(\lambda^2 - \lambda_k^2)^2 - 3\Gamma_k^2\lambda^2]}{[(\lambda^2 - \lambda_k^2)^2 + \Gamma_k^2\lambda^2]^3} \right\}, \tag{19}$$

$$\sigma(\lambda) = \sum_k \left\{ \frac{K^\sigma_{1k}\Gamma_k\lambda}{(\lambda^2 - \lambda_k^2)^2 + \Gamma_k^2\lambda^2} + \frac{K^\sigma_{2k}\Gamma_k\lambda^3(\lambda^2 - \lambda_k^2)}{[(\lambda^2 - \lambda_k^2)^2 + \Gamma_k^2\lambda^2]^2} + \frac{K^\sigma_{3k}\Gamma_k\lambda^5[3(\lambda^2 - \lambda_k^2)^2 - \Gamma_k^2\lambda^2]}{[(\lambda^2 - \lambda_k^2)^2 + \Gamma_k^2\lambda^2]^3} \right\}, \tag{20}$$

where new constants

$$\begin{aligned} &\Gamma_k = \gamma_0\lambda_k^2/\pi c,\ K^\rho_{1k} = AK^{(1)}_{k0}\lambda_k^2, \\ &K^\rho_{2k} = AK^{(2)}_{k0}\lambda_k^4/(2\pi c)^2,\ K^\rho_{3k} = AK^{(3)}_{k0}\lambda_k^6(2\pi c)^4 \text{ are used and} \\ &K^\rho_{1k} = K^\sigma_{1k},\ K^\rho_{2k} = 2K^\sigma_{2k},\ K^\rho_{3k} = K^\sigma_{3k};\ \lambda_k \end{aligned} \tag{21}$$

are the central dichroic wavelengths corresponding to the central dichroic frequencies ω_{k0}.

INTERPRETATION OF THE OPTICAL-ROTATORY DISPERSION EXPERIMENTAL DATA OF BENZIL

As has been mentioned previously, the theoretical optical-rotatory dispersion formula given by the solution of the three coupled oscillators model will be used. The optical-rotatory dispersion experimental data are approximated using the set of theoretical formulas, which are

single terms in the compound bracket on the right side of Eq. (19). Splitting Eq. (19), the following set of formulas is obtained:

$$\rho(\lambda) = \frac{K_{1k}^{\rho}(\lambda^2 - \lambda_k^2)}{(\lambda^2 - \lambda_k^2)^2 + \Gamma_k^2\lambda^2}, \tag{22}$$

$$\rho(\lambda) = \frac{K_{2k}^{\rho}\lambda^2[(\lambda^2 - \lambda_k^2)^2 - \Gamma_k^2\lambda^2]}{[(\lambda^2 - \lambda_k^2)^2 + \Gamma_k^2\lambda^2]^2}, \tag{23}$$

$$\rho(\lambda) = \frac{K_{3k}^{\rho}\lambda^4(\lambda^2 - \lambda_k^2)[(\lambda^2 - \lambda_k^2)^2 - 3\Gamma_k^2\lambda^2]}{[(\lambda^2 - \lambda_k^2)^2 + \Gamma_k^2\lambda^2]^3}. \tag{24}$$

The influence of these terms is manifested by the modification of the optical-rotatory dispersion curves, especially in the vicinity of the dichroic wavelengths, that is, in the vicinity of the absorption range. However, most experimental data of the optical-rotatory dispersion are measured in the wavelength region far from the absorption. In these cases the quantity Γ is zero or it has a small neglectable value, so that $(\lambda^2 - \lambda_k^2)^2 \gg \Gamma_k^2\lambda^2$ and the formulas (22)–(24) are reduced to the forms

$$\rho(\lambda) = \frac{K_{1k}^{\rho}}{\lambda^2 - \lambda_k^2}, \tag{25}$$

$$\rho(\lambda) = \frac{K_{2k}^{\rho}\lambda^2}{(\lambda^2 - \lambda_k^2)^2}, \tag{26}$$

$$\rho(\lambda) = \frac{K_{3k}^{\rho}\lambda^4}{(\lambda^2 - \lambda_k^2)^3}. \tag{27}$$

The formulas (25) and (26) are well known. The dependency given by Eq. (25) is known as the Drude formula and it [and also the formula (22), which is its generalization] plays a little role in the crystalline optical activity. The formula (26) was derived by Chandrasekhar [13].

The principle of the adjustment of the theoretical optical-rotatory dispersion formula is in general based on the minimization of the sum of squares

$$S = \sum_{n=1}^{N} T_n \left[\rho^{\exp}(\lambda_n) - \sum_{k=1}^{L}\sum_{j=1}^{3} \rho_{jk}^{\text{theor}}(\lambda_n, K_{jk}, \lambda_k, \Gamma_k)\right]^2, \tag{28}$$

where N is the number of the optical-rotatory dispersion experimental data measured for the wavelengths λ_n; $n = 1, 2, \ldots, N$; $\rho^{\exp}(\lambda_n)$ are the optical-rotatory dispersion experimental values, L is the number of central dichroic wavelengths used in the approximation, and the types of the terms for each central dichroic wavelength λ_k are denoted by the index j. The expression $\rho_{jk}^{\text{theor}}(\lambda_n, K_{jk}, \lambda_k, \Gamma_k)$ represents the result of each optical-rotatory dispersion term for the experimental wavelength λ_n, the central dichroic wavelength λ_k, and constants K_{jk} and Γ_k. The sum of squares (28) can contain the weight coefficients T_n by means of which the importance of the single experimental datum can be included. For example, by using these coefficients, the precision of the measurements of the single experimental datum can be considered. Recently we used the same method for the interpretation of experimental data of tellurium [18].

The initial theoretical optical-rotatory dispersion data in

$$\sum_{k=1}^{L} \sum_{j=1}^{3} \rho_{jk}^{\text{theor}}(\lambda_n, K_{jk}, \lambda_k, \Gamma_k), \tag{29}$$

that is, the number L of central dichroic wavelengths λ_k, the number and the types of the single theoretical terms for each λ_k, and also the initial values of λ_k and the constants K_{jk} and Γ_k have to be estimated. The final values of all these parameters are improved by the minimization of the sum of squares (28) using any proper minimization procedure. The residual value of the sum of squares is considered as the first criterion of the correctness of the used type of a formula in comparison with the residual sums of squares, which we obtain using other types of formulas. The second criterion is the physical reality of all computed values of the parameters. For example, the central dichroic wavelengths should lie inside the absorption region of the crystal, or the ratios of the constants K_{jk} for any k have to correspond to their definition given by the theory [17], for example, in the case of crystalline optical activity origin the absolute values of the constants K_{1k} and K_{3k} should be smaller than the absolute value of the constant K_{2k} and so forth.

The used unit of the optical-rotatory dispersion $\rho(\lambda)$ is $\text{deg} \cdot \text{mm}^{-1}$, the unit of λ is μm that is conventional. The used method of minimization of the sum of squares is the Marquardt–Levenberg method [19]. Using this method we obtained a very fast convergency of the sum of the least squares.

If the sum of squares is computed for the formula (4) with the experimental data of benzil given by Chandrasekhar [13] and Kizel et al. [10], the result gains the value $S = 9.58 \cdot 10^4$. This sum is

considered as a large value and the obtained theoretical formula can be qualified as insufficient.

Several possibilities of combinations of formula types (22), (23), and (24) were tested by the computer program VYSAG [20], which was designed for the interpretation of the optical-activity experimental data. The experimental data were measured for the wavelengths whose spacing is not equidistant. The weight coefficients T_n are chosen proportional to the size of intervals between neighboring measured values of wavelengths, therefore the sum of weight coefficients is equal to the number of experimental. The twelve-term formula

$$\rho(\lambda) = \frac{K_{11}^{\rho}}{\lambda^2 - \lambda_k^2} + \frac{K_{21}^{\rho}\lambda^2}{(\lambda^2 - \lambda_k^2)^2} + \frac{K_{31}^{\rho}\lambda^4}{(\lambda^2 - \lambda_k^2)^3} + \sum_{k=2}^{4}\left\{\frac{K_{1k}^{\rho}(\lambda^2 - \lambda_k^2)}{(\lambda^2 - \lambda_k^2)^2 + \Gamma_k^2\lambda^2} + \frac{K_{2k}^{\rho}\lambda^2[(\lambda^2 - \lambda_k^2)^2 - \Gamma_k^2\lambda^2]}{[(\lambda^2 - \lambda_k^2)^2 + \Gamma_k^2\lambda^2]^2} + \frac{K_{3k}^{\rho}\lambda^4(\lambda^2 - \lambda_k^2)[(\lambda^2 - \lambda_k^2)^2 - 3\Gamma_k^2\lambda^2]}{[(\lambda^2 - \lambda_k^2)^2 + \Gamma_k^2\lambda^2]^3}\right\}, \tag{30}$$

has been fit to the data to give minimal value of the sum of least squares $S = 834.4$. The central dichroic frequency $\lambda_1 = 0.2621\,\mu\text{m}$ corresponds with the short-wave absorption band; the frequencies $\lambda_2 = 0.3423\,\mu\text{m}$, $\lambda_3 = 0.3782\,\mu\text{m}$, and $\lambda_4 = 0.3949\,\mu\text{m}$ lie in the immediate vicinity of dichroic peaks. The aggregate entry of the result is made in Table 2. The graphical comparison of the experimental data and that given by our computation is presented by Figure 4.

The comparison of the available experimental circular dichroism data [9] with the theoretical circular dichroism curve is given by Eq. (20). This equation consists of three term types:

$$\sigma_{1k}(\lambda) = \frac{K_{1k}^{\sigma}\Gamma_k\lambda}{(\lambda^2 - \lambda_k^2)^2 + \Gamma_k^2\lambda^2}, \tag{31}$$

TABLE 2 Our Approximation of the Optical Rotatory Dispersion Experimental Data, $G = \sqrt{S/N} = 3.6\,\text{deg}\cdot\text{mm}^{-1}$

i	λ_i (μm)	K_{1i}^{ρ}	K_{2i}^{ρ}	K_{3i}^{ρ}	Γ_i (μm)
1	0.2621	−5.1834	10.0225	−0.0009	—
2	0.3423	–2.1436	0.1525	−0.0071	0.0265
3	0.3782	0.6827	0.1584	0.0275	0.0497
4	0.3949	−1.7541	−0.1594	0.0391	0.0516

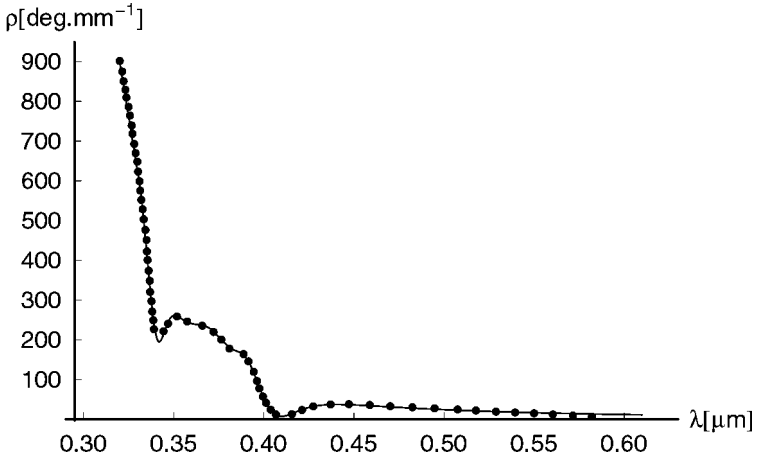

FIGURE 4 Graphical comparison of our result summarized in Table 2 with Kizel et al.'s [10] optical-rotatory dispersion experimental data of benzil crystal (points).

$$\sigma_{2k}(\lambda) = \frac{K_{2k}^{\sigma}\Gamma_k\lambda^3(\lambda^2 - \lambda_k^2)}{[(\lambda^2 - \lambda_k^2)^2 + \Gamma_k^2\lambda^2]^2}, \tag{32}$$

$$\sigma_{3k}(\lambda) = \frac{K_{3k}^{\sigma}\Gamma_k\lambda^5[3(\lambda^2 - \lambda_k^2)^2 - \Gamma_k^2\lambda^2]}{[(\lambda^2 - \lambda_k^2)^2 + \Gamma_k^2\lambda^2]^3}. \tag{33}$$

It has been previously proven that the corresponding terms ρ_{ik} and σ_{ik} are connected by the Kramers–Kronig transforms (2) and (3) on condition (21). For this reason, by substituting the values of constants K_{ik}^{σ}, Γ_k, and characteristic wavelengths λ_k from Table 2 to Eqs. (31)–(33), the circular-dichroism curve can be modeled.

The modeled circular-dichroism curve is mapped out in Figure 5. This theoretical result is compared with the experimental circular-dichroism data measured by Perekalina et al. [9]. Evidently the computed dichroic band at 0.3949 μm corresponds with the measured values. Because Perekalina's measurement was made for the wavelengths in the interval 0.340 μm–0.500 μm, the start of the second dichroic peak at 0.350 μm was observed. This peak was previously measured by Chaudhuri and El-Sayed [8] particularly because the higher-energy side of the spectrum had some degree of uncertainty

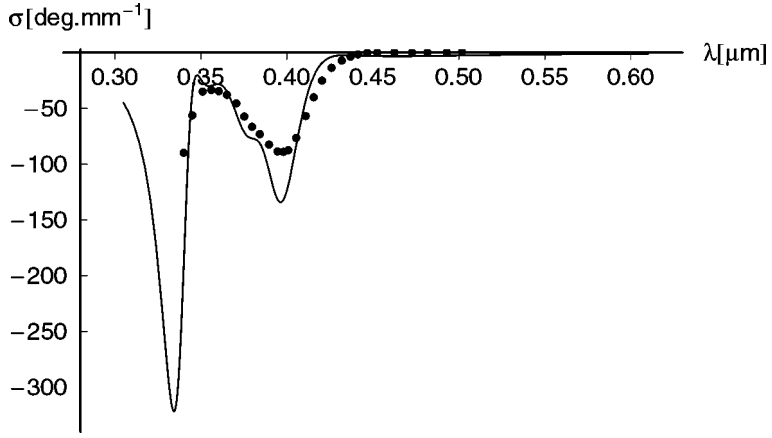

FIGURE 5 Graphical comparison of computed circular-dichroism curve (the solid line) and Perekalina et al.'s [9] circular-dichroism experimental data of benzil crystal (points).

caused by to an instrumental noise. The position of this band at 0.3325 μm corresponds very closely with the computed peak.

INTERPRETATION OF THE LATEST MEASUREMENT OF CIRCULAR-DICHROISM EXPERIMENTAL DATA OF BENZIL

Recently the solid-state circular-dichroism spectra were measured for the crystal of benzil [12]. The circular-dichroism spectra were obtained with freshly prepared KBr disks and recorded with a Jasco-715 dichrograph. The mixture of the sample and KBr was formed into a disk 0.5 mm thick and with radius of 15 mm.

Two samples were prepared for this purpose—one as a mixture of 1.33 mg of the benzil crystal and 320 mg of KBr (sample A), the other as a mixture of 3.2 mg of the benzil crystal and 260 mg of KBr (sample B). The circular dichroism exhibits an intense Cotton effect near 0.400 μm with a shoulder at 0.375 μm and a much weaker band of the same sign at 0.340 μm in both cases.

The number of 109 (sample A) and 104 (sample B) experimental values in the wavelength interval 0.330 μm–0.500 μm were chosen from this measurement. The result for the circular dichroism provided by the two coupled oscillator model [21] and then by the three coupled oscillator model [17] were used to be compared with the experimental data. As in the previous section, three dichroic wavelengths were considered and the weight coefficients were set $T_n = 1$.

TABLE 3 Approximation of the Circular Dichroism Experimental Data—sample A, $G = \sqrt{S/N} = 0.54$ mdeg

i	λ_i (μm)	K_{1i}^{ρ}	K_{2i}^{ρ}	K_{3i}^{ρ}	Γ_i (μm)
1	0.3360	0.3009	−0.0008	0.0013	0.0279
2	0.3731	1.6604	0.0247	0.0044	0.0371
3	0.4067	−3.7972	0.5898	0.0043	0.0845

At first the six-term formula

$$\sigma_{1k}(\lambda) = \sum_{k=1}^{3} \left\{ \frac{K_{1k}^{\sigma} \Gamma_k \lambda}{(\lambda^2 - \lambda_k^2)^2 + \Gamma_k^2 \lambda^2} + \frac{K_{2k}^{\sigma} \Gamma_k \lambda^3 (\lambda^2 - \lambda_k^2)}{[(\lambda^2 - \lambda_k^2)^2 + \Gamma_k^2 \lambda^2]^2} \right\} \tag{34}$$

was fitted to the data to minimize the sum of the least squares $S = 261.2$ for the sample A and $S = 940.3$ for the sample B. This formula consisting of the terms (31) and (32) is the result of the Chandrasekhar model of two coupled damped oscillators, which adjusted in our paper [21] and was used by Janku [22].

The usage of the nine-term formula

$$\sigma_{1k}\left(\lambda\right) = \sum_{k=1}^{3} \left\{ \frac{K_{1k}^{\sigma} \Gamma_k \lambda}{\left(\lambda^2 - \lambda_k^2\right)^2 + \Gamma_k^2 \lambda^2} + \frac{K_{2k}^{\sigma} \Gamma_k \lambda^3 \left(\lambda^2 - \lambda_k^2\right)}{\left[\left(\lambda^2 - \lambda_k^2\right)^2 + \Gamma_k^2 \lambda^2\right]^2} + \frac{K_{3k}^{\sigma} \Gamma_k \lambda^5 \left[3\left(\lambda^2 - \lambda_k^2\right)^2 - \Gamma_k^2 \lambda^2\right]}{\left[\left(\lambda^2 - \lambda_k^2\right)^2 + \Gamma_k^2 \lambda^2\right]^3} \right\}$$

provided by the approach to the crystalline optical activity by the model of three coupled oscillators minimizes the least squares considerably better: $S = 31.6$ for the sample A and $S = 202.6$ for the sample B. Tables 3 and 4 show this result for both samples. The graphical comparison of experimental data and computed theoretical curves is presented in Figures 6 and 7.

DISCUSSION

It was shown that the theoretical connection of the optical-rotatory dispersion and circular dichroism as the real and imaginary part of

TABLE 4 Approximation of the Circular Dichroism Experimental Data—Sample B, $G = \sqrt{S/N} = 1.39$ mdeg

i	λ_i (μm)	K^{ρ}_{1i}	K^{ρ}_{2i}	K^{ρ}_{3i}	Γ_i (μm)
1	0.3365	0.5359	−0.0037	0.0019	0.0259
2	0.3734	4.0851	0.0724	0.0124	0.0383
3	0.4031	−9.6101	1.0710	0.0999	0.0800

the complex rotatory power (1) by the Kramers–Kronig transforms (2) and (3) can be considered to be valid for the particular case of the optical-rotatory dispersion and circular-dichroism data of the benzil crystal. Therefore, the optical-rotatory dispersion curve gives us important information about the circular-dichroism curve, although the circular dichroism was not measured.

The only differences are in the maximum circular-dichroism value of every peak and in the widths of the bands. These differences are not large. They could be the result of various samples of benzil crystal used by Kizel et al. [10] and Perekalina et al. [12]. In particular, the preparation methods of samples or their thicknesses differed. Perekalina et al.'s [12], Chaudhuri and El-Sayed's [8], and Kizel et al.'s [10] measurements were also realized at different temperatures. Chaudhuri and El-Sayed [8] performed the experiment at 77 K; unfortunately Perekalina et al. [9] did not specify the temperature.

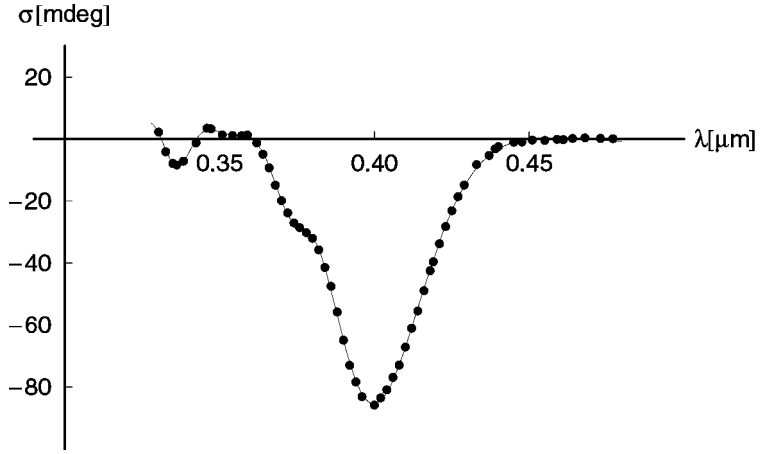

FIGURE 6 Graphical comparison of our result summarized in Table 3 with circular-dichroism experimental data of benzil crystal—sample A (points) [12].

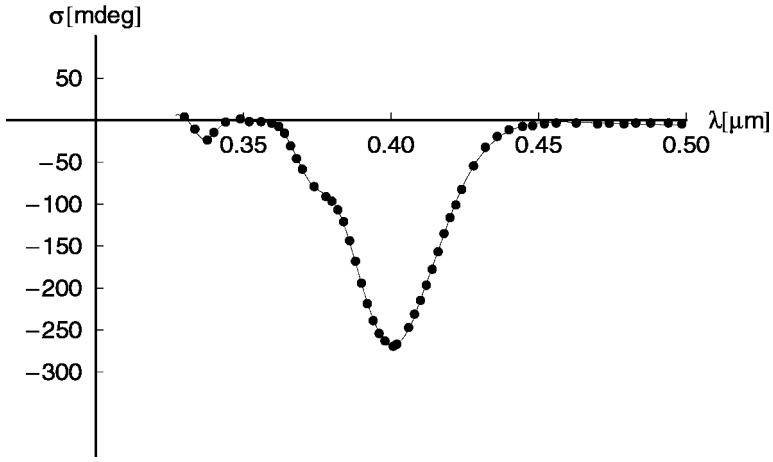

FIGURE 7 Graphical comparison of our results summarized in Table 4 with circular-dichroism experimental data of benzil crystal—sample B (points) [12].

Although benzil molecules are optically inactive in solution, they may be expected to contribute considerably to the optical activity of crystalline benzil because of their geometry (see Fig. 1). The absence of the optical activity in solution can be caused by a small value of the potential barrier between leavorotatory and dextrorotatory forms of these molecules. This leads to a fast racemization, which is restrained by the potential field of the benzil crystal.

The wavelength dependence derived for the optical-rotatory dispersion and circular dichroism of molecules [7] or for delocalized molecular aggregates [23] corresponds to the terms (22) and (31). The description of the crystalline optical activity using the two coupled oscillators model provides the sum of terms (22) and (23) for the optical-rotatory dispersion and (31) and (32) for the circular dichroism. The terms (24) and (33) are added to the optical-rotatory dispersion and circular dichroism respectively using the three coupled oscillators model.

The previous results [9,13] and our computations showed that the optical-rotatory dispersion of benzil crystal cannot be modeled by the only first (22) or by the sum of the first (22) and the second (23) terms satisfactorily. The addition of the third term (24) is necessary, although the term of type (22) plays a dominant role in this results and the influence of the molecular optical activity is appreciable.

A similar situation is observed in the case of the recently measured circular dichroism spectra of benzil crystal with KBr disks. The

discrepancy between the experiment and calculation can be described by the quantity $G = \sqrt{S/N}$ (S is the sum of squares, N the number of experimental data), which represents the average difference between the experimental and calculated values. This average difference is close to the level of inaccuracy of the measurement and therefore is not of a systematic nature. Conversely if the third term (33) is not contributed, the average difference increases threefold.

This result is not specific to benzil crystals only. Recently the importance of the third term (24) was proven for the optical-rotatory dispersion of tellurium [18], where the experimental data provided by Brown and Forsyth [24] were analyzed. A similar successful result was obtained for the circular-dichroism peak of sodium uranyl acetate crystal in the wavelengths range from 0.47304 μm to 0.47359 μm [17].

The comparison of approximations of the circular-dichrosim experimental data measured by Perekalina et al. [9] and the new data provided by Polonski et al. [12] shows that all central dichroic wavelengths do not differ substantially. Conversely, the Cotton effect observed by Polonski et al. [12] at 0.340 μm is much weaker than the peak at the same wavelength obtained by Perekalina et al. [9]. This discrepancy leads to the conclusion that this band could be attributed to the transition in the benzoyl moiety [12,25], whereas Chaudhuri and El-Sayed [8] expected that the peak is caused by the second $n - \pi^*$ transition resulting from the intramolecular interaction of the two carbonyl groups of the benzoyl units in the benzil molecule.

REFERENCES

[1] Allen, N. C. B. (1927). *Phil. Mag.*, *3*, 1037.
[2] Banerjee, K. & Sinha, N. L. (1937). *Indian J. Phys.*, *11*, 409.
[3] Brown, S. J. & Sadanaga, R. (1965). *Acta Cryst.*, *18*, 158.
[4] More, M., Odou, G., & Lefebvre, J. (1987). *Acta Cryst.*, *B43*, 398.
[5] Chandrasekhar, S. (1954). *Proc. Indian Acad. Sci.*, *A39*, 243.
[6] Kizel, V. A., Krasilov, Y. I., & Shamraev, V. N. (1964). *Opt. i Spectroscopiya*, *17*, 470 [English transl. (1964). *Opt. Spectroscopy*, *17*, 863].
[7] Moffitt, W. & Moscowitz, A. (1959). *J. Chem. Phys.*, *30*, 648.
[8] Chaudhuri, N. K. & El-Sayed, M. A. (1967). *J. Chem. Phys.*, *47*, 1133.
[9] Perekalina, Z. B., Kaldybaev, K. A., Konstantinova, A. F., & Belyaev, L. M. (1977). *Sov. Phys. Crystallogr.*, *22*, 556.
[10] Kizel, V. A., Krasilov, Y. I. & Shamraev, V. N. (1969). *Spectroscopy of Solid Matter* (in Russian), *4*, 85.
[11] Moxon, J. R. L., Renshaw, A. R., & Tebbutt, I. J. (1991). *J. Phys. D: Appl. Phys.*, *24*, 1187.
[12] Polonski, T., Szyrszyng, M., Gdaniec, M., Nowak, E., & Herman, A. (2001). *Tetrahedron: Asymmetry*, *12*, 797.
[13] Chandrasekhar, S. (1961). *Proc. Roy. Soc.*, *A259*, 531.
[14] Říha, J., Sváčková, K., & Vyšín, I. (1998). *Acta UPOL Physica*, *37*, 99.

[15] Cohen-Tannoudji, C., Diu, B., & Laloe, F. (1992). *Quantum Mechanics*. Wiley: Paris.
[16] Dawydow, A. S. (1981). *Quantenmechanik*. VEB Deutsche Verlag der Wissenschaft: Berlin.
[17] Vyšín, I., Sváčková, K., & Říha, J. (2000). *Opt. Commun.*, *174*, 455.
[18] Vyšín, I., Sváčková, K., & Říha, J. (2002). *Appl. Cryst.*, *35*, 96.
[19] Marquardt, D. W. (1963). *Soc. Indust. Appl. Math.*, *11*, 431.
[20] Vyšín, I. (2000). *Acta UPOL Physica*, *39*, 41.
[21] Vyšín, I. & Říha, J. (1998). *Acta UPOL Physica*, *37*, 77.
[22] Janků, V. (1969). *Optica Acta*, *16*, 225.
[23] Wagersreiter, T. & Mukamel, S. (1996). *J. Chem. Phys.*, *105*, 7995.
[24] Brown, P. J. & Forsyth, J. B. (1996). *Acta Cryst.*, *A52*, 408.
[25] Polonski, T. & Dauter, Z. (1986). *J. Chem. Soc., Perkin Trans. 1*, 1781.